Validity of Pressure-Velocity Correction Algorithm (C-HSMAC method) for Incompressible Fluids with Passive Scalar Convection

AUTHOR(S):

Ushijima, S.; Tanaka, H.; Toriu, D.

J. Adv. Simulat. Sci. Eng.
Vol. 6, No. 1, 260–272.

Validity of Pressure-Velocity Correction Algorithm (C-HSMAC method) for Incompressible Fluids with Passive Scalar Convection

S. Ushijima[1*], H. Tanaka[2], D. Toriu[1]

[1]ACCMS, Kyoto University, Japan
[2] Faculty of Engineering, Kyoto University, Japan

*ushijima.satoru.3c@kyoto-u.ac.jp

Received: November 1, 2018; Accepted: May 7, 2019; Published: May 30, 2019

Abstract. In the computations of incompressible fluids, it is essentially important to obtain accurately the velocity components that satisfy the incompressible condition ($\nabla \cdot \boldsymbol{u} = 0$) as well as the pressure variables which are consistent with the velocity fields. For this purpose, a pressure-velocity correction method (C-HSMAC method) has been proposed by Ushijima et al. (2002) with a finite volume method (FVM) for incompressible fluids. The purpose of this paper is to estimate the effects of the unsatisfied incompressible condition on the passive scalar convection and to confirm that the C-HSMAC method is able to suppress them. The C-HSMAC and usual SMAC methods were applied to the passive scalar convection in the cavity having an oscillating top wall. It was concluded that the unsatisfied incompressible condition may cause the unphysical scalar overshoots in the SMAC method. In contrast, the C-HSMAC method enables us to control $|\nabla \cdot \boldsymbol{u}|$ with the given threshold ϵ_D and to suppress such overshoots. In addition, it was demonstrated that the C-HSMAC method allows us to obtain reasonable results without overshoots even in combination with a higher-order scheme for convection terms with finer cell divisions.

Keywords: Incompressible fluid, Velocity divergence, Pressure-velocity correction, C-HSMAC method, Passive scalar convection

1. Introduction

In the computations of incompressible fluids, it is essentially important to obtain the velocity components that satisfy the incompressible condition ($\nabla \cdot \boldsymbol{u} = 0$) accurately as well as the pressure variables which are consistent with the velocity fields. It has been shown that the non-negligible numerical errors due to the unsatisfied incompressible condition cause the unphysical change of volumes of the fluid during the unsteady computations [1] as well as the unphysical overshoots of scalar variables that will be shown in this paper. It is noted that

the numerical errors arising from the unsatisfied incompressible conditions are substantially different from the inherent compressibility of the actual fluid properties.

In order to suppress such numerical errors and to control the divergence of velocity vector $\boldsymbol{u}$ so that $|\nabla \cdot \boldsymbol{u}| < \epsilon_D$ can be established with a given threshold ϵ_D, which is not possible by the usual numerical algorithms for incompressible fluids like a simplified MAC (SMAC) method [2], the pressure-velocity correction algorithm (C-HSMAC method) has been proposed and confirmed its effectiveness in the preceding studies [1, 3, 4]. Although the similar computation method that is able to control $\nabla \cdot \boldsymbol{u}$ was proposed as a HSMAC or SOLA method [5] in 1980, it has also been shown that the computational efficiency of the C-HSMAC method is much better than the HSMAC or the SOLA method in our previous study [6].

The purpose of this paper is to estimate the effects of the unsatisfied incompressible condition on the passive scalar convection by incompressible fluids. Thus, the C-HSMAC and usual SMAC methods are applied to the same passive scalar convection in the cavity having an oscillating top wall. From the comparisons of computational results, it is shown that the unphysical overshoots occur in the calculated passive scalar when the incompressible condition is not adequately satisfied with the SMAC method. In contrast, it is confirmed that the C-HSMAC method enables us to control $|\nabla \cdot \boldsymbol{u}|$ in each fluid cell with the given threshold ϵ_D and that the unphysical overshot scalar can be suppressed. Finally, it is demonstrated that the scalar convection is reasonably predicted with the C-HSMAC method even in combination with a higher-order scheme, for example a third-order total variation diminishing (TVD) scheme [7], for convection terms with finer cell divisions.

2. Numerical procedures

2.1. Governing equations

The governing equations for an isothermal and incompressible Newtonian-fluid are given by the following incompressible condition and Navier-Stokes equations respectively:

$$\frac{\partial u_i}{\partial x_i} = 0 \tag{1}$$

$$\frac{\partial u_i}{\partial t} + \frac{\partial (u_i u_j)}{\partial x_j} = -\frac{1}{\rho}\frac{\partial p}{\partial x_i} + \nu \frac{\partial^2 u_i}{\partial x_j^2} \tag{2}$$

In addition, the following convection equation of passive scalar c is dealt with in this study:

$$\frac{\partial c}{\partial t} + \frac{\partial (c u_j)}{\partial x_j} = 0 \tag{3}$$

where t is time, x_i is the $i-$component of the orthogonal coordinates, u_i is the velocity component in x_i direction, ρ is density, p is pressure and ν is kinematic viscosity. In this study, ρ and ν are constants. All dependent and independent variables in this paper are non-dimensional.

The passive scalar c can be thought of as any physical variable, such as the normalized concentration of solution without diffusion or the color function used in VOF methods, any of which are in the range of $0 \leq c \leq 1$. In case that c is used as the color function, the results obtained in this study give us useful information for the surface tracking between gas and liquid phases. Since one of the merits in the present method is that the calculation of c is conducted with a finite volume method (FVM), the conservation of mass or volume in incompressible fluids is sufficiently satisfied in contrast to most of the other surface tracking methods. In addition, the unphysical numerical oscillations can be suppressed when using the C-HSMAC method as concluded in this paper.

2.2. Discretization and computational procedures

The governing equations are discretized with a finite volume method (FVM) in the collocated grid system [8] as illustrated in Fig. 1. In contrast to the staggered grid system, all variables are defined at the cell center points as shown in Fig. 1. While the convection and diffusion terms are calculated at the cell-center points, the cell-center velocity components are spatially interpolated on the cell boundaries in the pressure calculations in order to prevent velocity-pressure coupling oscillations [8].

The merits of the collocated grid system are that it can be used in the unstructured meshes [8] and that it is easy to implement the domain decomposition method for parallel computations in distributed-memory systems. In fact, the C-HSMAC method has been developed in the unstructured tetrahedron cells [9] as well as been parallelized with the domain decomposition method [10].

In this study, the two-dimensional uniform rectangular cells are used as shown in Fig. 1 to make the problems simple. The variables, $u_{c,i}$, p and c, are all defined at the cell-center points, while cell-boundary velocity components $u_{b,i}$ are also used to estimate the mass, momentum and scalar fluxes on the cell boundaries.

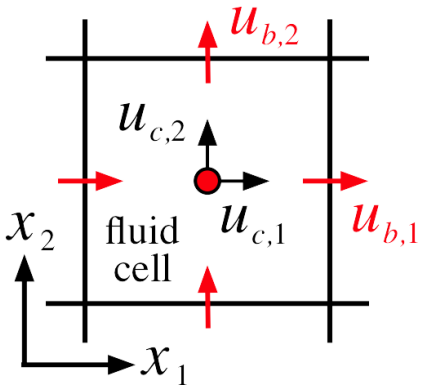

Figure 1: Fluid cell in 2D collocated grid system

For simplicity, the governing equations, which are discretized only in the time direction with a first-order semi-implicit method, are shown to explain the outline of the numerical procedures. The unknown variables u_i^{n+1} and p^{n+1} satisfy the following equation:

$$u_i^{n+1} = u_i^n - \frac{1}{\rho}\frac{\partial p^{n+1}}{\partial x_i}\Delta t + F_i^n \Delta t \tag{4}$$

where superscripts n and $n+1$ stand for the time steps and Δt is the time increment. The convection and diffusion terms are included in F_i^n as

$$F_i^n = -\frac{\partial (u_i^n u_j^n)}{\partial x_j} + \nu \frac{\partial^2 u_i^n}{\partial x_j^2} \tag{5}$$

Meanwhile, we can calculate the tentative velocity component u_i^* with the following equation using p^n:

$$u_i^* = u_i^n - \frac{1}{\rho}\frac{\partial p^n}{\partial x_i}\Delta t + F_i^n \Delta t \tag{6}$$

Subtracting Eq. (6) from Eq. (4), the following equation is derived:

$$u_i^{n+1} = u_i^* - \frac{1}{\rho}\frac{\partial \phi}{\partial x_i}\Delta t \tag{7}$$

where

$$\phi = p^{n+1} - p^n \tag{8}$$

On the other hand, u_i^{n+1} need to satisfy the incompressible condition given by

$$\frac{\partial u_i^{n+1}}{\partial x_i} = 0 \tag{9}$$

With Eq. (9) the partial derivative of Eq. (7) with respect to x_i becomes

$$\frac{\partial^2 \phi}{\partial x_i^2} = \frac{\rho}{\Delta t}\frac{\partial u_i^*}{\partial x_i} \tag{10}$$

Since the right hand side of Eq. (10) is already calculated, ϕ can be easily obtained by solving the spatially-discretized Eq. (10), which corresponds to a pressure-Poisson equation, with some matrix solvers. After ϕ is obtained, u_i^{n+1} and p^{n+1} are calculated from Eq. (7) and Eq. (8) respectively.

The convection equation of scalar c, given by Eq. (3), is also discretized with a finite volume method in a rectangular fluid cell as shown in Fig. 1. The scalar fluxes cu_i are estimated on cell boundaries using the velocity components $u_{b,i}$ located on the boundaries so that the scalar c can be conserved in each fluid cell.

2.3. C-HSMAC method

In the pressure computation procedure, in which Eq. (10) is solved, the following C-HSMAC method [1] is used in order to obtain the velocity components that satisfy the incompressible condition as well as the pressure variables consistent with the velocity components. In this method, the following iterative calculation is conducted:

do $k = 1, 2, \cdots, k_m$

$$\frac{\partial^2 \phi}{\partial x_i^2} = \frac{\rho}{\Delta t} \frac{\partial u_{b,i}^k}{\partial x_i} \tag{11}$$

$$p^{k+1} = p^k + \phi^k \tag{12}$$

$$u_{b,i}^{k+1} = u_{b,i}^k - \frac{\Delta t}{\rho} \frac{\partial \phi^k}{\partial x_i} \tag{13}$$

$$\text{exit if} \quad \frac{\partial u_{b,i}^{k+1}}{\partial x_i} < \epsilon_D \ \text{ in all cells} \tag{14}$$

enddo

In the above equations, $u_{b,i}$ is the cell-boundary velocity, as shown in Fig. 1, which is estimated from the spatial interpolation of $u_{c,i}$ defined at the cell-center point in the collocated grid system. The superscripts k and $k+1$ stand for the iterative number of the C-HSMAC method. The initial values $u_{b,i}^1$ are given as u_i^* calculated at the cell-center point. The threshold that controls the divergence of the velocity vector is given by ϵ_D.

It is noted that the threshold ϵ_ϕ, which is used to solve the linear system of ϕ, needs to be decreased according to the iterative steps of the C-HSMAC method [1]. To maintain this condition, ϵ_ϕ at $k-$th iteration of the C-HSMAC method may be set like $\epsilon_{\phi,k} = \alpha_\phi^k \epsilon_{\phi,0}$, where the parameter α_ϕ is in the range of $0 < \alpha_\phi < 1$ (i.e. $\alpha_\phi^{k+1} < \alpha_\phi^k$ is established where k is exponent) and $\epsilon_{\phi,0}$ is an initial threshold. Thus, the threshold $\epsilon_{\phi,k}$ becomes smaller as the number of iteration number increases. This numerical procedure on the thresholds is due to the fact that the errors of incompressible conditions $|\nabla \cdot \boldsymbol{u}|$ are related to the residuals of the linear system of ϕ, which was mathematically derived in our previous paper [10].

After the iterative computations of the C-HSMAC method, $|\nabla \cdot \boldsymbol{u}| < \epsilon_D$ is established in all fluid cells in the computational domain. However, the usual SMAC method [2], which corresponds to the C-HSMAC method without the above iteration (i.e. $k_m = 1$), is unable to control $|\nabla \cdot \boldsymbol{u}|$ directly by such threshold. In the following section, the threshold for Eq. (11) in the SMAC method is denoted by $\epsilon_{\phi,0}$, since $k_m = 1$ in the SMAC method.

In summary, the usual SMAC method cannot control the incompressible condition $\nabla \cdot \boldsymbol{u} = 0$ directly. Instead, the incompressible condition is indirectly controlled through the linear system of ϕ. Thus, some trials and errors are necessary to determine the suitable threshold $\epsilon_{\phi,0}$ for the linear system of ϕ. In contrast, the C-HSMAC method monitors $|\nabla \cdot \boldsymbol{u}|$ in each cell every computational step so that $|\nabla \cdot \boldsymbol{u}|$ can be less than the given threshold ϵ_D, which is the essential merit of the C-HSMAC method.

3. Passive scalar convection calculated with C-HSMAC method

3.1. Conditions of computations

In order to demonstrate the validity of the C-HSMAC method, it is applied to the passive scalar convection due to an incompressible fluid in a cavity with an oscillating upper wall.

Figure 2 shows the initial distributions of the passive scalar in a square cavity, in which all side lengths are 1.0. The orthogonal coordinates are defined as shown in Fig. 2. In the initial conditions, the fluid is static and the scalar c is set at 1.0 in $x_2 \geq 0.5$ and 0.0 in $x_2 < 0.5$ respectively. The velocity U of the oscillating top wall is given by $U = \cos(2\pi t)$ as shown in Fig. 2. On the other wall boundaries, non-slip conditions are imposed on the velocity, while $\partial p/\partial n = 0$ and $\partial c/\partial n = 0$ are given on all boundaries. The kinematic viscosity ν is set at 1.0×10^{-2} in the following computations.

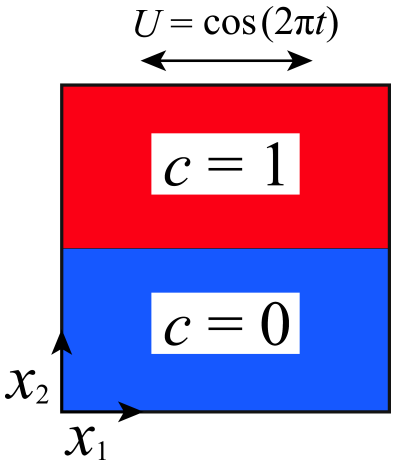

Figure 2: Computational area and initial scalar distributions

In the following part of the present study, the thresholds and the related parameter in pressure computations are set as follows: $\epsilon_{\phi,0} = 1.0 \times 10^{-3}$ for both C-HSMAC and SMAC methods, while in the C-HSMAC method $\epsilon_D = 1.0 \times 10^{-10}$ and $\alpha_\phi = 0.1$ with sufficiently large k_m to obtain the converged results in the iterative calculations. To solve the linear system of ϕ, which are derived from the discretization of Eq. (11), the Bi-CGSTAB [11] method is used in both C-HSMAC and SMAC methods.

3.2. Overshoots of scalar due to unsatisfied incompressible conditions

In the unsteady computations of the passive scalar convection as shown in Fig. 2, the maximum value of c should be less than or equal to 1.0, since there are no source terms in the convection equation of c given by Eq. (3) and no incoming nor outgoing scalar fluxes through the boundaries of the closed cavity. The convected scalar, however, is not calculated adequately in case that the non-negligible numerical errors arise in the calculated results for the incompressible condition defined by Eq. (9).

In this section, it will be shown that the unphysical overshoots of c may arise, which means that the scalar larger than 1.0 appears in the calculated results, when the SMAC method is used with the threshold $\epsilon_{\phi,0}$ as written above. In addition, it is also demonstrated that such unphysical overshoots can be suppressed by using the C-HSMAC method.

In the calculations, in order to prevent the numerical oscillations, which might arise from

higher-order schemes for convection terms, a simple first-order upwind method is used to estimate the momentum and scalar fluxes on cell boundaries which need to be calculated in the FVM. Thus, the calculated results for c should be included in the range of $0.0 \leq c \leq 1.0$, when the velocity components are adequately obtained. The number of fluid cells is 20×20 in x_1 and x_2 directions respectively. The time increment Δt is 2.0×10^{-2} and unsteady computations were conducted until $t = 10.0$. It is noted that since the top wall oscillates with the velocity $U = \cos(2\pi t)$ as shown in Fig. 2, the scalar distributions are not always symmetric in the process of the unsteady computations.

In the first time step from the initial conditions, from $t = 0.0$ to $t = \Delta t$, the 20 iterative calculations were conducted in the C-HSMAC method to satisfy the given thresholds described above. The elapsed computational time was about 1.27×10^{-2} [sec] in the first time step of the computation. The total elapsed time until $t = 10.0$ was about 5.81 [sec]. These elapsed computational times were measured by a serial computation with the Intel Xeon Broadwell 2.1GHz processor. All calculations in this paper were performed with serial numerical procedures, while the parallelized C-HSMAC method has already been implemented in a three-dimensional computation method by Ushijima et. al. [10].

Figure 3 shows the time histories of c_{max}, which is the maximum c in all computational area shown in Fig. 2. As shown in Fig. 3, the maximum values of c_{max} in the SMAC method are about 7% of the initial $c_{max} = 1.0$, while no overshoots are found and c_{max} is kept nearly 1.0 throughout the computations in case of the C-HSMAC method.

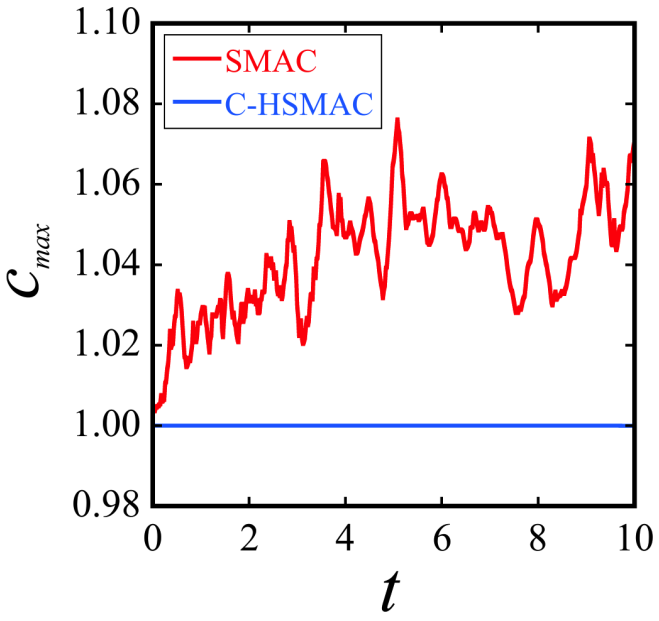

Figure 3: Time histories of maximum c with first-order upwind method (number of fluid cells = 20×20)

It is thought that the overshoots found in the SMAC method in Fig. 3 are caused by the numerical error due to the fact that the incompressible condition is not accurately satisfied. Figure 4 (a) shows the distributions of the area where overshoots occur in the SMAC method at $t = 3.0$. In Fig. 4 (a) c_{err} is the overshooting values from the initial $c_{max} = 1.0$ defined by

$$c_{err} = 100\,(c - 1.0) \qquad [\text{if } c > 1.0 \text{ otherwise } c_{err} = 0.0] \tag{15}$$

As shown in Fig. 4 (a), the large overshoots occur near the upper right corner. Figure 4 (b) shows the distribution of $\nabla \cdot \boldsymbol{u}$ calculated with the SMAC method at $t = 3.0$. While $\nabla \cdot \boldsymbol{u}$ ought to be almost zero in the incompressible fluid, relatively large positive values appear near the upper right corner of the cavity, where the large overshoots are found in Fig. 4 (a).

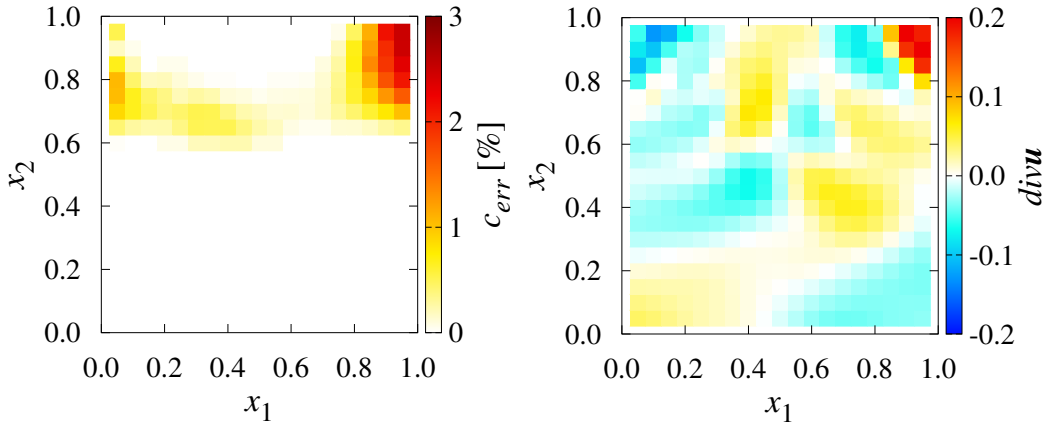

(a) Distribution of c_{err} (b) Distribution of $\nabla \cdot \boldsymbol{u}$

Figure 4: Distributions of c_{err} and $\nabla \cdot \boldsymbol{u}$ calculated with first-order upwind method and SMAC method ($t = 3.0$, number of fluid cells $= 20 \times 20$)

On the other hand, in case of the C-HSMAC method, $\nabla \cdot \boldsymbol{u}$ is directly controlled with the given threshold $\epsilon_D = 1.0 \times 10^{-10}$, so that $|\nabla \cdot \boldsymbol{u}|$ should be less than ϵ_D. Actually, the range of $\nabla \cdot \boldsymbol{u}$ is from -2.45×10^{-11} to 3.69×10^{-11} at $t = 3.0$, which is sufficiently small compared with the result of the SMAC method as shown in Fig. 4 (b). In addition, regarding the distribution of c_{err}, no overshoots are found at $t = 3.0$. Throughout the unsteady computation with the C-HSMAC method, the maximum value of the overshoot is 3.92×10^{-12} in the whole computational domain. This value is negligible compared with the results of the SMAC method shown in Fig. 4 (a). Therefore, it can be said that the C-HSMAC method is effective to prevent the overshoots of the passive scalar convection.

From the above results, it is expected that the numerical error in $\nabla \cdot \boldsymbol{u}$ is closely related to the overshoots of c_{max}. In the following part, more detailed relationship between $\nabla \cdot \boldsymbol{u}$ and the overshoots of c_{max} will be discussed.

For simplicity, let us consider the transportation of scalar c in the fluid cell located at the upper right corner of the computational area as illustrated in Fig. 5. In this fluid cell, just two fluxes, which are indicated as q_1 and q_2 in Fig. 5, are related to the increase or decrease

rate of c_2. This is written as the following discretized equation:

$$\frac{c_2^{n+1} - c_2^n}{\Delta t}\Delta x_1 \Delta x_2 = q_1 \Delta x_2 - q_2 \Delta x_1 \tag{16}$$

where Δx_1 and Δx_2 are lengths of the rectangular fluid cell in x_1 and x_2 directions respectively.

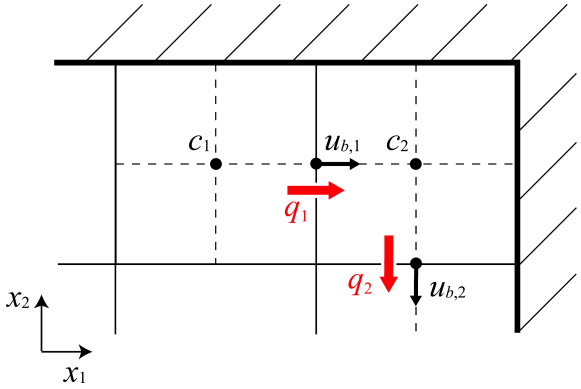

Figure 5: Configuration of variables in fluid cell located at upper right corner

In case that the directions of velocity components $u_{b,1}$ and $u_{b,2}$ are given as shown in Fig. 5, the fluxes q_1 and q_2 are estimated with the upwind method as $q_1 = c_1 u_{b,1}$ and $q_2 = c_2 u_{b,2}$ respectively. At the beginning of computations, the scalar in the upper region is expected to be near 1.0 taking account of the initial condition shown in Fig. 2. Thus, when we assume that $c_1^n = c_2^n = 1.0$, Eq. (16) is rewritten as

$$c_2^{n+1} = 1 + \frac{\Delta t}{\Delta x_1 \Delta x_2} D \tag{17}$$

where D corresponds to the divergence of the velocity vector in the fluid cell given by

$$D = u_{b,1}\Delta x_2 - u_{b,2}\Delta x_1 \tag{18}$$

Thus, D should sufficiently be close to zero in the incompressible fluid. However, if D takes a non-negligible positive value rather than near-zero value, c_2^{n+1} in Eq. (17) becomes larger than 1.0, which results in the overshot estimation. This fact indicates that the estimation of velocity components that satisfy the incompressible condition accurately is essentially important to prevent the overshoots of the passive-scalar calculations. Therefore, it can be concluded that the C-HSMAC method is effective to calculate passive-scalar computations, since this method allows us to control the divergence of velocity vectors in all fluid cells with the given threshold ϵ_D.

3.3. Calculations of scalar distributions with TVD scheme

In the above section 3.2, it was confirmed that the unphysical overshoots of passive scalar occur due to the unsatisfied incompressible conditions and that the overshoots can be suppressed by the C-HSMAC method. In section 3.2, a simple first-order upwind method was used in the computation of passive scalar in order to exclude the possibility that the numerical oscillations arise from the higher-order schemes used to calculate convection terms. The purpose of this section is to demonstrate that the reasonable results for passive scalar without overshoots can be obtained even in combination with a higher-order scheme for convection terms with finer cell divisions.

In the calculations of convection terms included in Eqs. (2) and (3) with the FVM, the momentum and scalar fluxes are estimated on the fluid-cell boundaries with the third-order total variation diminishing (TVD) scheme [7]. In addition, the number of fluid cells is set at 100×100 and the time increment Δt is 2.0×10^{-3}.

In the pressure computations, both SMAC and C-HSMAC methods are used to compare the results of c_{max}. Figure 6 shows the time histories of c_{max} in the present computations. In case of the C-HSMAC method in Fig. 6, no overshoots are found and c_{max} is kept at around 1.0. However, when using the SMAC method, overshoots still arise as shown in Fig. 6, which are caused by the same reason as the results shown in Fig. 3 obtained with a first-order upwind method. From these results in Fig. 6, it can be seen that the C-HSMAC method is effective when using the third-order TVD scheme in the finer 100×100 cells.

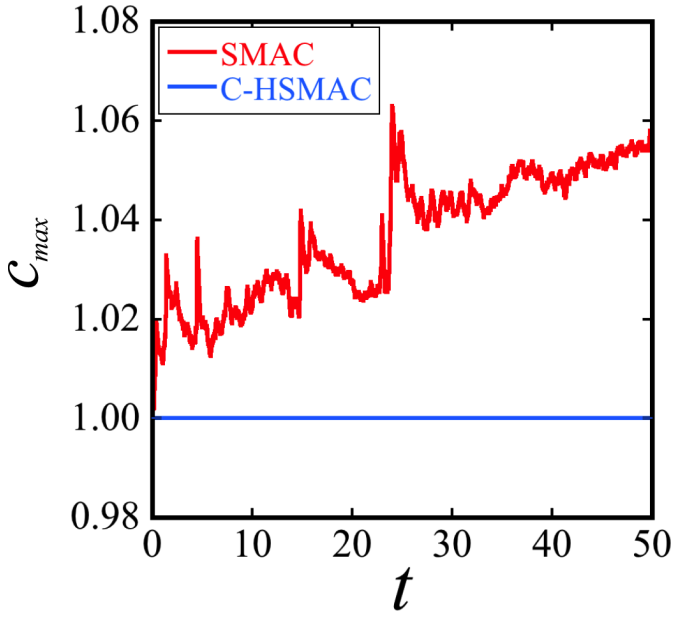

Figure 6: Time histories of maximum values of c with TVD scheme (number of fluid cells = 100×100)

Finally, the computational results obtained with the C-HSMAC method will be shown. Figure 7 shows the distributions of the velocity vectors at the thinned points from the actual 100×100 fluid cells. It can be seen that the flows due to the top wall movements occur only in the upper area of the cavity, since $\nu = 0.01$ and the Reynolds number is small; $Re = |U/\nu| \leq 100$. As shown in Fig. 7, the clockwise and counterclockwise flows occur periodically depending on the direction of the movement of the upper wall.

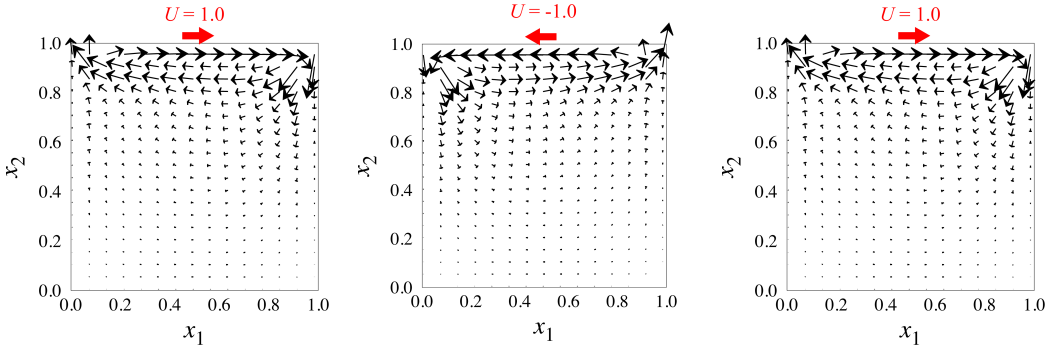

(a) $t = 10.0$ (b) $t = 30.5$ (c) $t = 50.0$

Figure 7: Velocity vectors calculated with TVD scheme and C-HSMAC method (number of fluid cells = 100×100)

Figure 8 shows the distributions of the passive scalar at $t = 10.0$, 30.5 and 50.0, which were calculated with the third-order TVD scheme and the C-HSMAC method using 100×100 fluid cells. As the flows in the upper region of the cavity develop due to the oscillating top wall, the scalar initially located in the lower region is lifted up from near the center of the interface at $t = 10.0$ to 30.5 and then it reaches the top boundary at $t = 50.0$ as observed in Fig. 8. It can be seen that the behavior of passive scalar is adequately calculated without unphysical overshoots and with keeping a sharp interface between two scalar values.

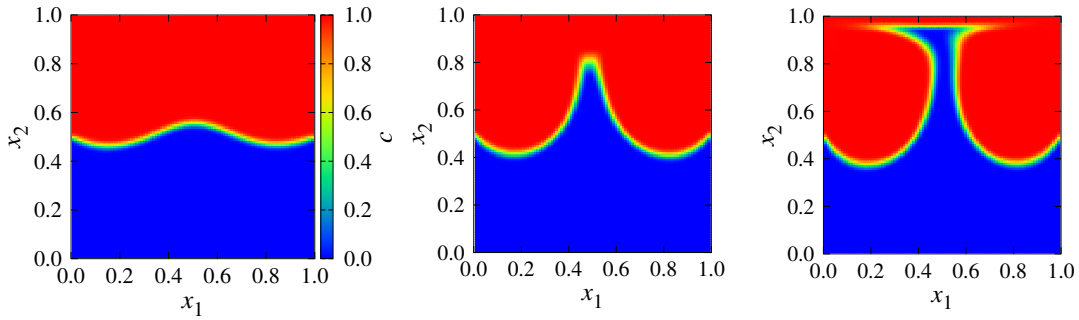

(a) $t = 10.0$ (b) $t = 30.5$ (c) $t = 50.0$

Figure 8: Distribution of passive scalar c calculated with TVD scheme and C-HSMAC method (number of fluid cells = 100×100)

4. Conclusions

In the computations of passive scalar convected by incompressible fluids, it is essentially important to obtain the velocity components that satisfy the incompressible condition ($\nabla \cdot \boldsymbol{u} = 0$) as well as the pressure variables which are consistent with the velocity fields. In this study, the effectiveness of the pressure-velocity correction algorithm (C-HSMAC method), has been demonstrated for passive scalar convection, since the C-HSMAC method enables us to obtain velocity and pressure fields that satisfy incompressible conditions correctly.

To discuss the effects of the unsatisfied incompressible conditions, the C-HSMAC and usual SMAC methods were applied to the passive scalar convection in the cavity having the oscillating top wall. As a result, it was shown that when the incompressible condition is not adequately satisfied with the SMAC method, the unphysical overshoots occur in the calculated results of the passive scalar. Thus, such numerical errors possibly arise in case that the usual SMAC method is applied to pressure computations for the incompressible fluids with an inappropriate threshold $\epsilon_{\phi,0}$. In contrast, it was demonstrated that the C-HSMAC method enables us to control $|\nabla \cdot \boldsymbol{u}|$ in each fluid cell with the given threshold ϵ_D and that the unphysical overshoots of scalar can be suppressed by the C-HSMAC method. In addition, it was shown that the computational results of scalar convection in the cavity have no overshoots with the C-HSMAC method even in combination with a higher-order scheme, which is a third-order TVD scheme as an example in this paper, for convection terms with finer cell divisions.

One of the deficits of the usual SMAC method and other similar algorithms for incompressible fluids is that they cannot control the incompressible condition $\nabla \cdot \boldsymbol{u} = 0$ directly. Instead, this incompressible condition in these methods is indirectly controlled through the linear system of ϕ. From that reason, some trials and errors are necessary to determine the suitable threshold $\epsilon_{\phi,0}$ for the linear system of ϕ which needs not a little manpower. If the excessively strict threshold $\epsilon_{\phi,0}$ is given, the computational time may much larger than that of the C-HSMAC method. In contrast, the C-HSMAC method monitors $|\nabla \cdot \boldsymbol{u}|$ in each cell every computational step so that $|\nabla \cdot \boldsymbol{u}|$ can be less than the given threshold ϵ_D, which is the notable merit of the C-HSMAC method. In this paper, it was demonstrated that the C-HSMAC method allows us to suppress the unphysical overshoots arising in the computations of passive scalar caused by the unsatisfied incompressible conditions.

References

[1] S. Ushijima, I. Nezu, and M. Sanjou: Computational method for Navier-Stokes equations accompanied by free-surface deformation. *Proc. 12th International Offshore and Polar Engineers*, 2002, 223–239.

[2] A. A. Amsden and F. H. Harlow: A simplified MAC technique for incompressible fluid flow calculations. *J. Comp. Phys.*, 6 (1970), 322–325.

[3] S. Ushijima: Multiphase-model to predict arbitrarily-shaped objects moving in free surface flows. *Proc. 18th International Offshore and Polar Engineers*, 2008, 621–628.

[4] S. Ushijima and N. Kuroda: Numerical prediction of shielding effects on fluid-forces acting on complicated-shaped object. *Journal of applied mechanics JSCE*, 11 (2008), 769–778.

[5] B. D. Nichols, C. W. Hirt, and R. S. Hotchkiss: SOLA-VOF : A solution algorithm for transient fluid flow with multiple free boundaries. *Los Alamos Scientific Laboratory Report, LA-8355*, 1980.

[6] S. Ushijima and Y. Okuyama: Comparison of C-HSMAC and SOLA methods for pressure computation of incompressible fluids. *JSCE Journal*, 747:II-65 (2003), 197–202.

[7] S. Yamamoto and H. Daiguji: Higher-order-accurate upwind schemes for solving the compressible Euler and Navier-Stokes equations. *Computers & Fluids*, 22:2–3 (1993), 259–270.

[8] C. M. Rhie and W. L. Chow: Numerical study of the turbulent flow past an airfoil with trailing edge separation. *AIAA Journal*, 21 (1983), 1525–1532.

[9] S. Ushijima, Y. Okuyama, M. Fujita, and I. Nezu: C-HSMAC method for incompressible flows with unstructured collocated grid system. *J. Applied Mech. JSCE*, 7 (2004), 347–354.

[10] S. Ushijima, Y. Okuyama, and I. Nezu: Implicit computational algorithm for 3D incompressible flows with collocated grid system and its parallelization. *J. Applied Mech. JSCE*, 6 (2003), 185–192.

[11] H. A. Van Der Vorst: Bi-CGSTAB : A fast and smoothly converging variant of Bi-CG for the solution of nonsymmetric linear systems. *SIAM J. Sci. Stat. Comput.*, 13 (1992), 631–644.